ANALYSIS AND SIMULATION OF THE MAST (COFS-I FLIGHT HARDWARE)

Lucas G. Horta, Joanne L. Walsh, Garnett C. Horner
NASA Langley Research Center
Hampton, Virginia

and

James P. Bailey
PRC - Kentron
Hampton, Virginia

First NASA/DOD CSI Technology Conference
November 18-21, 1986

INTRODUCTION

The Control of Flexible Structures (COFS) program involves ground and flight tests of large flexible space structures such as the one shown in figure 1. The MAST (COFS-I) flight experiment is the initial phase of this program. An overview of the program is presented in references 1 and 2. The program includes the design and fabrication of 60 meter deployable truss with sensors and actuators attached at pre-selected locations. The structure will be used in a multi-flight experimental program to understand the dynamic behavior of joint-dominated structures, to supply a test bed for the implementation of modern control algorithm for vibration suppression, and to perform on/off line system identification.

This paper presents some of the in-house analysis work performed to evaluate the proposed design configuration, controller design as well as actuator dynamic modeling, and MAST/actuator dynamic simulation for excitation and damping. The MAST is modeled using the Engineering Analysis Language (EAL, ref. 3) finite element analysis program. An optimization procedure which minimizes weight while trying to maintain modal coupling is discussed. This optimization procedure facilitates incorporation of additional constraints not considered in the MAST baseline design. Mode shapes from EAL are used to construct a reduced order model of the MAST for closed-loop simulation. Details on the proposed actuator location, number, and characteristics are discussed as well as some of the alternate ways to use them. Simple rate feedback laws are implemented to show the viability of the proposed experiment. Complete simulation includes excitation and damping using the same set of actuators.

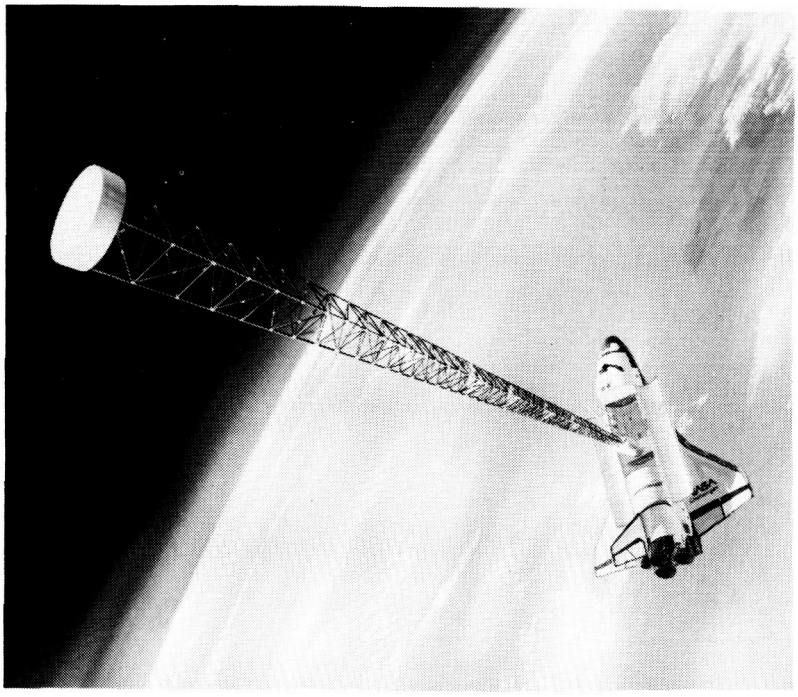

Figure 1

MAST FINITE ELEMENT MODEL

The finite element model (FEM) of the MAST is shown in figure 2. The truss beam is 60 meters long and consists of 54 bays of single-laced latticed beams. The longerons which form the vertices of the triangular cross-sections have unequal areas resulting in one strong and two weak longerons. The strong longeron is aligned with the centerline of the Shuttle axis. The longerons and diagonals are modeled using tube elements. The model includes the deployer retractor assembly, Shuttle inertia properties (modeled with beam elements), rigid platforms for sensors and actuators allocation, and a parameter modification package. There are three secondary actuator locations distributed along the beam (bays 12, 30, and 44) and one primary at the tip. Each of the secondary actuator stations contains two actuators acting in the same plane. The primary station has four actuators to impart torques as well as in-plane forces. Also included are two sensor measurement stations (bays 24 and 48) for the implementation of non-collocated control laws. At the beam tip, in addition to the actuators, a parameter modification package composed of four masses constrained to move along a track are used to vary the structure center of mass. These four masses can be independently operated to achieve high modal coupling. The FEM also contains lumped masses at each joint location and cable mass for the electronic components distributed along the beam.

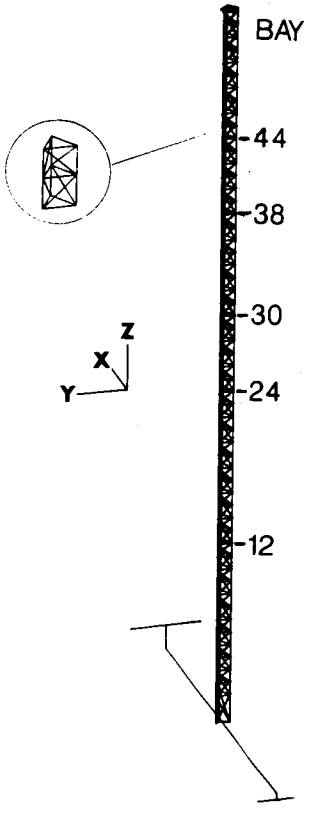

Figure 2

MAST BEAM DESCRIPTION

Table 1 shows the beam properties used in the FEM of the baseline design. Note that the longerons which form the vertices of the cross-section triangle have different cross-sectional areas in order to promote coupling between the bending and torsion modes.

TABLE 1 - FLIGHT MAST BEAM DESCRIPTION

GEOMETRY		
Diameter		1.40 m
Bay Length		1.12 m
Number of Bays		54
Strong Longeron (1)	OD/ID	0.0220/0.0104 m
Weak Longeron (2)	OD/ID	0.0229/0.0147 m
Diagonal	OD/ID	0.0191/0.0179 m
Batten	OD/ID	0.0140/0.0114 m
EFFECTIVE AXIAL STIFFNESS OF MEMBERS (EA)		
Strong Longeron (1)		39.10 E+06 N
Weak Longeron (2)		33.60 E+06 N
Diagonal		3.86 E+06 N
Batten		6.64 E+06 N
MASS SUMMARY		
Corner Joint Mass		0.9072 kg
Roll Nut (every other bay)		0.52 kg
Diagonal Mid-Hinge		0.30 kg
Cabling (distributed to each bay) Total		4.0 kg
Deployer Retractor Assembly		720.0 kg
Actuator Wts at Bays 12,30,44		18.8 kg
Tip Mass Assembly		73.0 kg
Parameter Modification Package (4 masses, 20 kg ea)		80.0 kg

Note: Data from MAST FLIGHT SYSTEM CODR held at Harris Corp, Melbourne, FLA. 4/29 to 5/4/86.

EIGENVALUES AND MODE SHAPES OF MAST FINITE ELEMENT MODEL

Table 2 shows the first ten eigenvalues of the baseline FEM without the actuator masses. The third column shows the bending axis. The corresponding first four mode shapes are shown in figure 3. The bays which contain actuators or sensors are indicated by tic marks to show how effective the actuator stations are with regard to the mode shapes. Note, for example, that for the second bending mode, bay 30 and the tip are the most effective.

TABLE 2 - FINITE ELEMENT MODEL EIGENVALUES

Mode Number	Frequency (Hz)	Direction
1	.1888	1BY
2	.2414	1BX
3	1.291	2BX
4	1.338	1T
5	1.339	2BY
6	3.686	3BX
7	3.831	3BY
8	4.303	2T
9	6.713	4BX
10	6.946	4BY

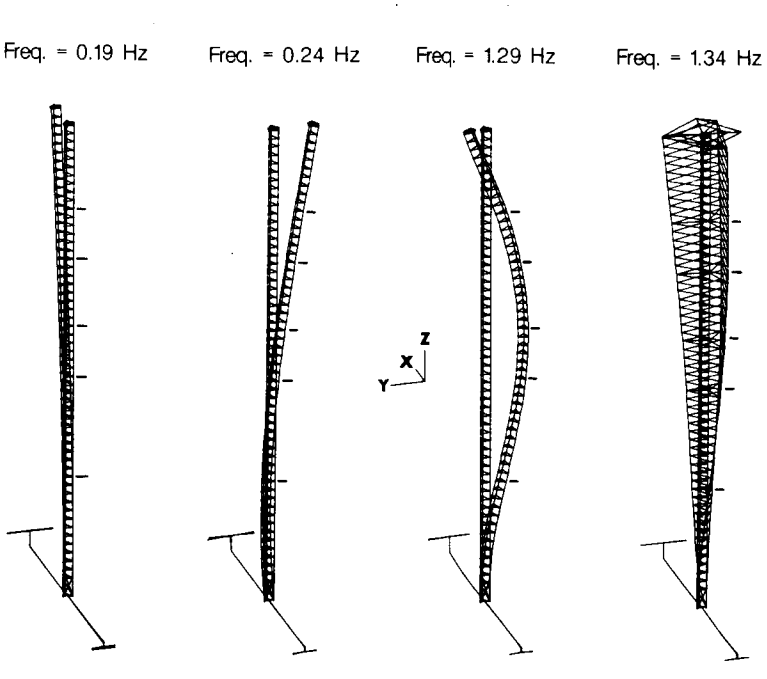

Figure 3

OPTIMIZATION FORMULATION

An optimization procedure which uses the baseline FEM has been developed in order to incorporate additional requirements not considered in the baseline design - namely, that the first bending frequency of the diagonal must be at least 15 Hz. The optimization procedure combines a general purpose optimization program (CONMIN, ref. 4) with the EAL finite element program. The problem formulation is shown in figure 4. The objective is to minimize the total mass of the system. The four design variables are the inner radii of the strong and weak longeron (R_S and R_W, respectively) and the inner and outer radii of the diagonal (R_I and R_O, respectively). The following constraints are imposed on the problem: the lowest natural frequency of the MAST must be greater than 0.18 Hz (a Shuttle requirement); the first torsion and the second bending frequencies must be within 1 percent (referred to as modal coupling); the first bending frequency of the diagonal must be at least 15 Hz (to simulate a buckling constraint); the inner radius of the weak longeron must be at least 0.25 mm larger than the inner radius of the strong longeron (to ensure that the weak and strong longerons do not change); and the minimum wall thickness of the diagonal must be at least 0.56 mm. The lower bound for all the design variables is 3.175 mm and the upper bound is 9.4 mm with the exception of the diagonal outer radius which is 11 mm.

- OBJECTIVE FUNCTION - MINIMIZE TOTAL MASS
- DESIGN VARIABLES
  - INNER RADIUS OF WEAK LONGERON, R_W
  - INNER RADIUS OF STRONG LONGERON, R_S
  - INNER RADIUS OF DIAGONAL, R_I
  - OUTER RADIUS OF DIAGONAL, R_O
- CONSTRAINTS
  - 1ST NATURAL FREQUENCY OF MAST $\geq$ 0.18 Hz
  - 1ST TORSION AND 2ND BENDING FREQUENCY WITHIN 1%
  - 1ST NATURAL FREQUENCY OF DIAGONAL $\geq$ 15 Hz
  - $R_W - R_S \geq 0.25$ mm
  - WALL THICKNESS OF DIAGONAL $\geq$ 0.56 mm

Figure 4

OPTIMIZATION RESULTS - OBJECTIVE FUNCTION AND DESIGN VARIABLES

Plots of the mass (objective function) and the design variables versus design cycles are shown in figure 5. The baseline design of the MAST is used as the initial design (design cycle = 0). Over the design process, the mass increases by 40 kg over the baseline design. The design variables associated with the longerons (R_W and R_S) decrease from the baseline design values with the inner radius of the strong longeron (R_S) reaching its lower bound. The design variables associated with the diagonal (R_I and R_o) increase from the baseline design values with the inner radius R_I reaching its upper bound. The reason for the increase in the objective function and the trends in the design variables will be discussed in the following.

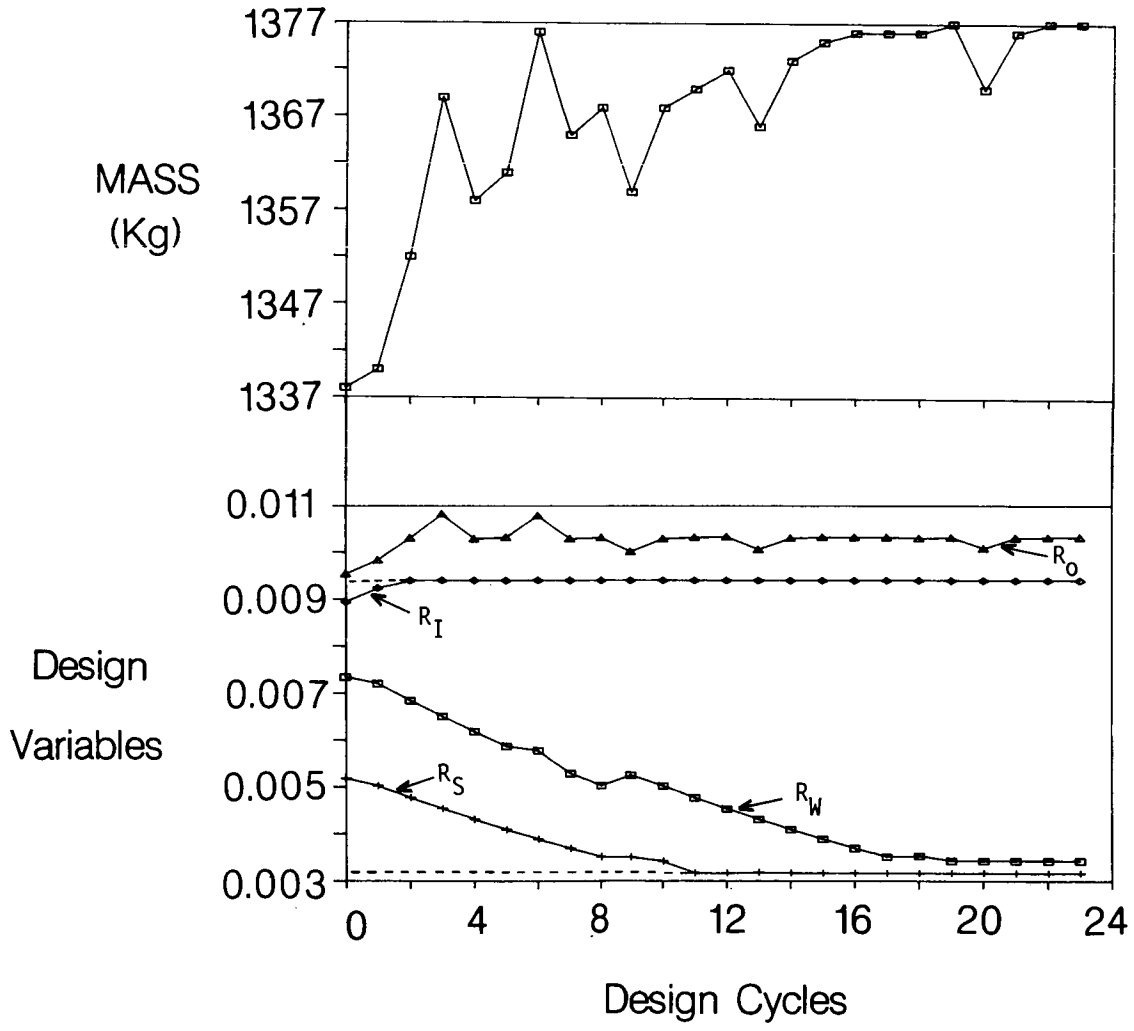

Figure 5

OPTIMIZATION RESULTS - CONSTRAINTS

As shown in figure 6, the baseline design satisfies all the design requirements except the diagonal frequency constraint (greater than 15 Hz). In general, the diagonal wall thickness (R_o-R_I, upper plot) increases as the diagonal frequency increases (middle plot). The constraints on the diagonal frequency and on the weak and strong longerons (R_W-R_S) are the active constraints causing the objective function to increase. The first torsion mode frequency is highly affected by the diagonal member stiffness. The diagonal frequency constraint is equivalent to the diagonal stiffness for small member mass changes. Thus when the diagonal frequency is increased, the torsion frequency is also increased. This causes the modal coupling and the diagonal frequency constraints to work against each other. When the first torsion and second bending frequencies are within 1 percent (lower plot), the diagonal frequency (middle plot) is less than 15 Hz (see cycles 13 and 20). When the diagonal frequency is 15 Hz, the modal coupling constraint is not satisfied. Since it is a MAST requirement to have coupled modes, alternative formulations of the optimization problem are being explored which will lead to the simultaneous satisfaction of both constraints. One formulation being investigated is to have the modal coupling as the objective function.

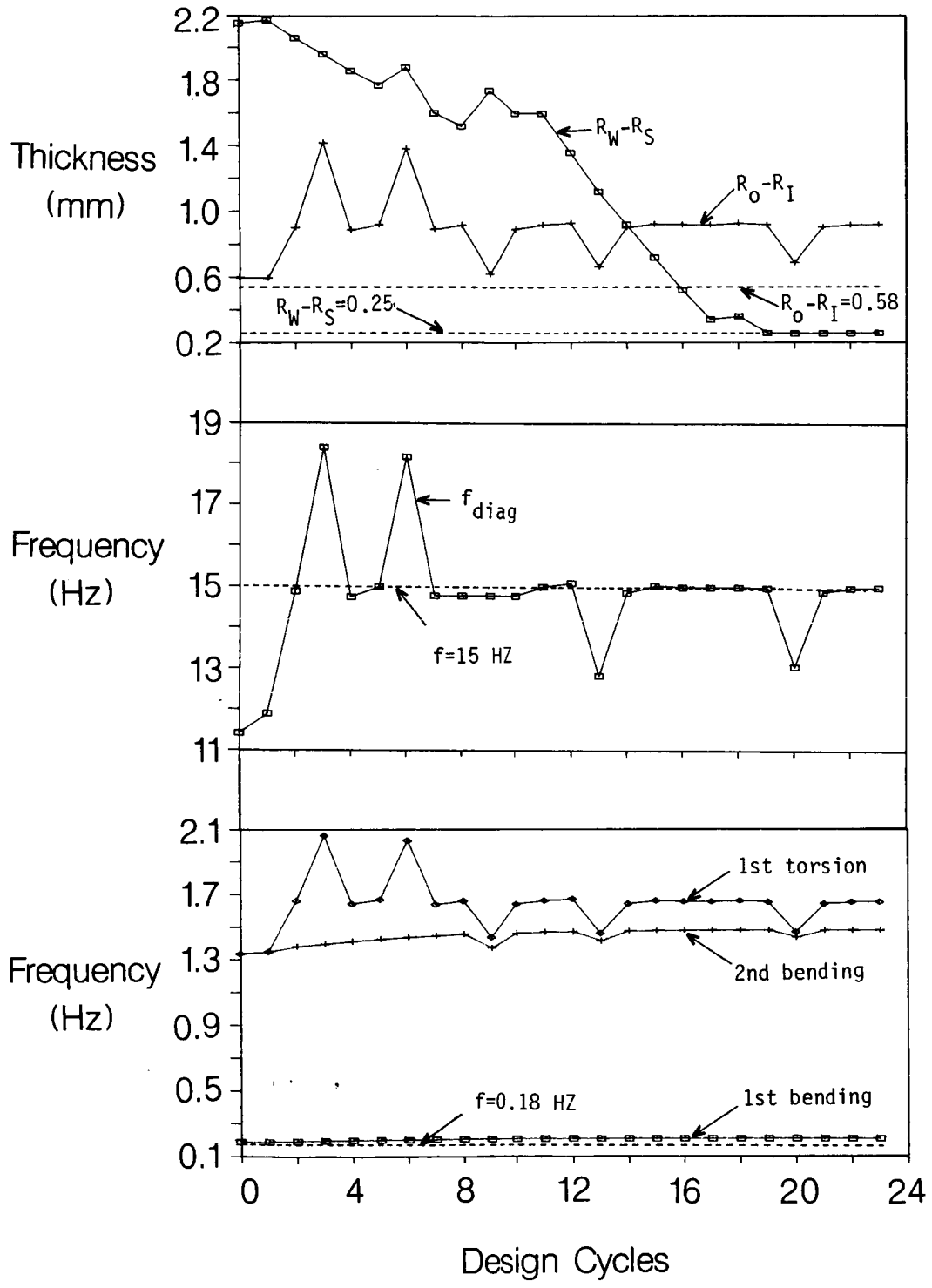
Thickness
(mm)
2.2
1.8
1.4
1.0
0.6
0.2
R_W-R_S
R_o-R_I
R_W-R_S=0.25
R_o-R_I=0.58
Frequency
(Hz)
19
17
15
13
11
f_{diag}
f=15 HZ
Frequency
(Hz)
2.1
1.7
1.3
0.9
0.5
0.1
1st torsion
2nd bending
f=0.18 HZ
1st bending
0
4
8
12
16
20
24
Design Cycles

Figure 6

LINEAR DC MOTOR (LDCM) ACTUATOR

The photograph shown in figure 7 is the prototype Linear DC Motor (LDCM) actuator built by Harris Corporation to be used on the MAST.

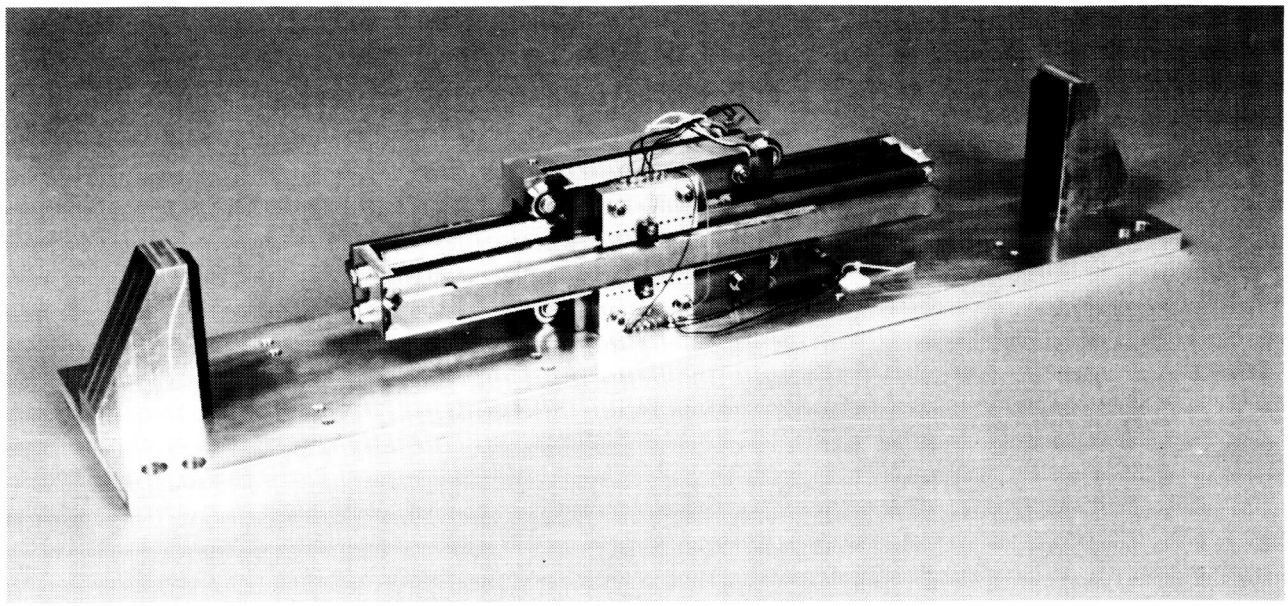

Figure 7

ACTUATOR MODELING

Actuator modeling brings out several design issues that need to be addressed. Physically, the actuator is an electromechanical device which can be commanded in a number of different ways. Using the actuator representation shown in figure 8 (the structure deflection is denoted by W whereas the actuator position is defined by Y), the equations of motion are as shown. The designer must decide how the actuators will be used and, moreover, what type of command input the actuator will require. For the system shown, Fa is the force applied to the structure which is balanced by accelerating the actuator mass in the opposite direction. When commanded a force, the actuator mass should accelerate until the desired force is achieved (assuming no stroke limits). If commanded a position, the actuator will move either relative to the structure or with respect to an inertial reference. Deciding how the actuator is used determines instrumentation needs. Moreover, deciding how it operates (position of force command) determines the actuator representation. The following work presents one of the available options.

Representation

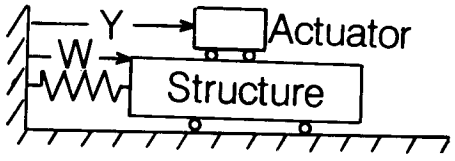

Equations of Motion

Structure

$$M \ddot{W} + k W = F a$$

Actuator

$$m \ddot{Y} = -F a$$

Issues

- Position Command
- Force Command
- Actuator Representation

Figure 8

DYNAMIC MODEL OF ACTUATOR

The dynamic model of the actuator used in this study is based on the work presented in references 5 and 6. The schematic in figure 9 shows the actuator main components. The actuator mass is denoted by m_p, stiffness K_p, damping (back EMF) c_p, and the commanded force f_g. The commanded force acts directly between the actuator and the structure. In this schematic, the structure is represented as a single spring-mass system M_s and K_s. Looking at the operation of such a device, if K_p and c_p are zero and the actuator is commanded a constant force, the actuator mass will accelerate in one direction (ideally). In this dynamic model the centering spring K_p forces the actuator mass back to a nominal position. Since such a spring does not exist, this operation is to be performed by local position feedback. The operational frequency defined as $\omega_p = \sqrt{K_p/m_p}$ divides the operational range of the actuators into two basic regions. This will be discussed in the following.

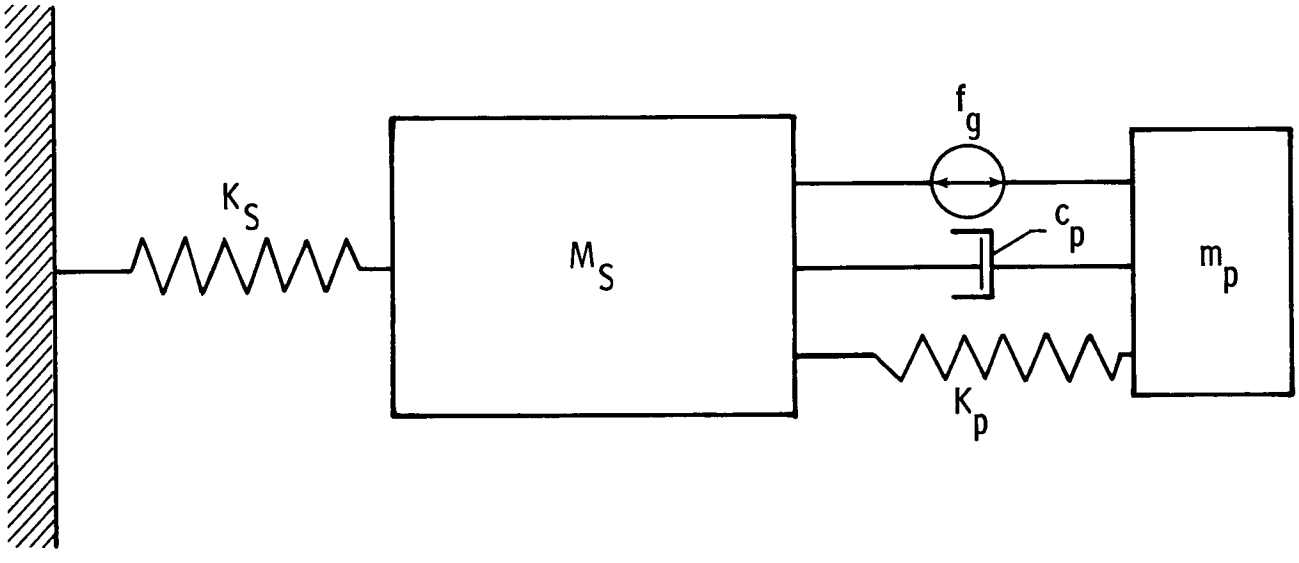

Figure 9

ACTUATOR FREQUENCY RESPONSE

The dynamic characteristics of the actuator model are better described by the frequency response plots shown in figure 10. These frequency response functions were obtained from a bench test of the actuator reported in reference 5. Although this actuator design is different from the LDCM design, they are conceptually similar. Moreover, the actuator dynamic model can be assumed the same for simulation. The upper plot shows the transfer function of the total actuator output force to the input commanded voltage. Note that the commanded voltage can be equal to any desired control. The frequency response function shown resembles that of a second-order high pass filter where above the operational frequency the response is "independent" of frequency. Moreover, above the operational frequency, defined in the dynamic model as ω_p, the output force follows the input command (see phase plot) whereas below ω_p the output is out-of-phase with the input. This is extremely important when the actuator is used for control. For example, if flexible structural modes exist on both sides of ω_p and the commanded input contains rate information from multiple modes, then in the lower modes the actuator is adding energy whereas in the higher modes it is removing energy. The operational frequency parameter is an adjustable parameter to some extent by adjusting K_p. This actuator model is used for the MAST dynamic simulation.

ACTUATOR FREQUENCY RESPONSE—MAGNITUDE

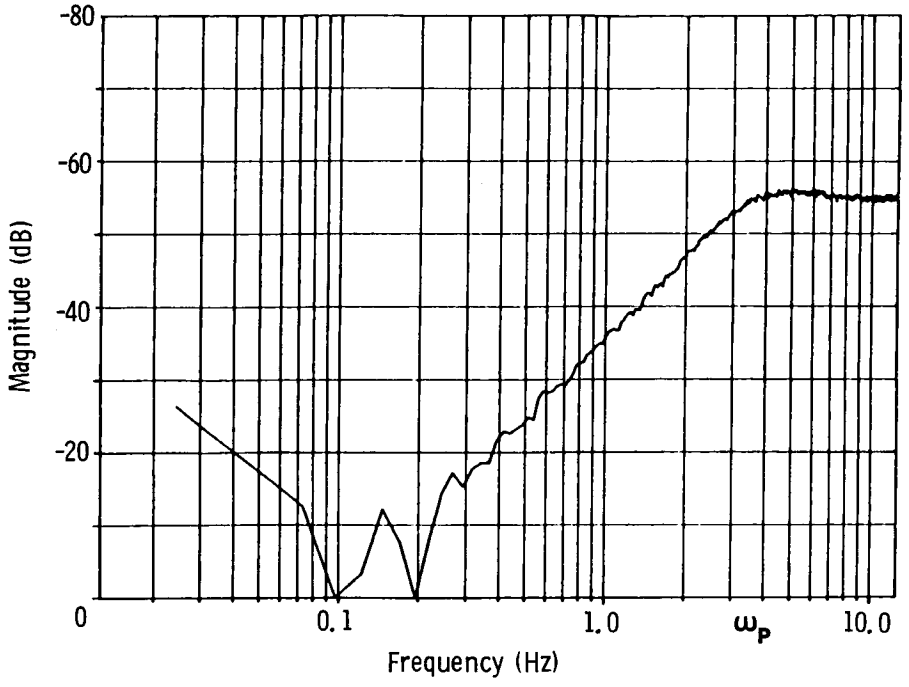

ACTUATOR FREQUENCY RESPONSE—PHASE

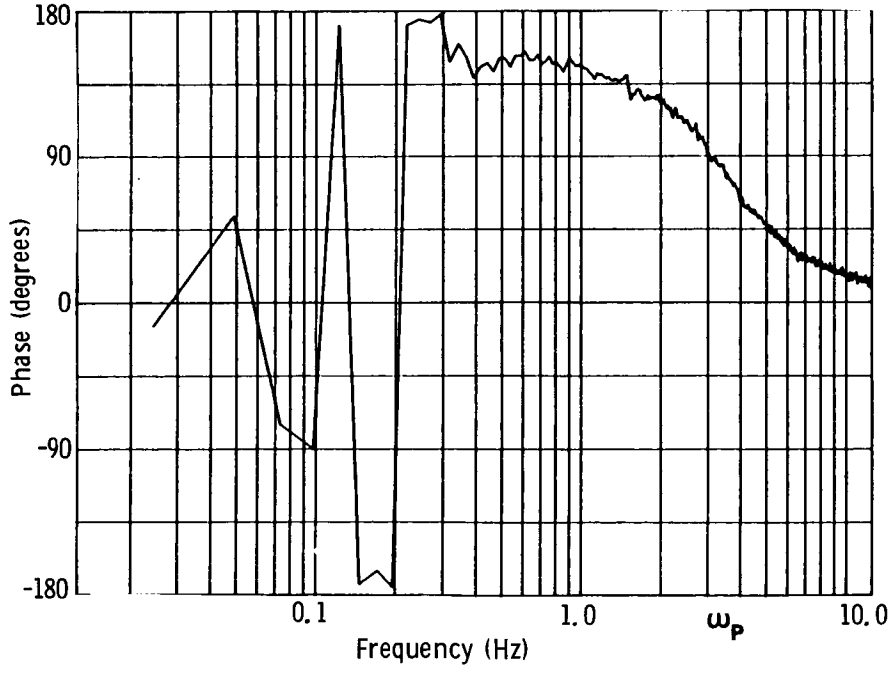

Figure 10

MAST DYNAMIC SIMULATION

The dynamic model of the actuator is incorporated into a reduced order model of the MAST. This model contains 6 rigid body modes and 10 flexible modes. A total of ten actuators are present but only the tip actuators are used in this simulation. The proposed MAST flight experiment as envisioned involves three phases - excitation, free vibration (dwelling), and control (damping). A test sequence is simulated where the same set of actuators is used for excitation and damping of the beam. For excitation the commanded force to the actuator is $f_g = \sin \omega t$. The frequency is that of the first bending mode 0.19 Hz. For control the commanded force is proportional to the beam rate $f_g = C \dot{W}$. The proportionality constant C is obtain by pole placement of the first two bending modes to achieve 5 percent modal damping. The actuator operational frequency is set to 0.1 Hz. The simulated tip response is shown in the upper plot of figure 11 and the corresponding actuator stroke output in the lower plot. A complete sequence (excitation, dwell, and damping) is presented. The excitation f_g is turned-off after a beam deflection of 10 cm is reached (t=60.4 sec). The beam is allowed to vibrate freely for 20 seconds and the control is turned-on for the last 30 seconds of the simulation.

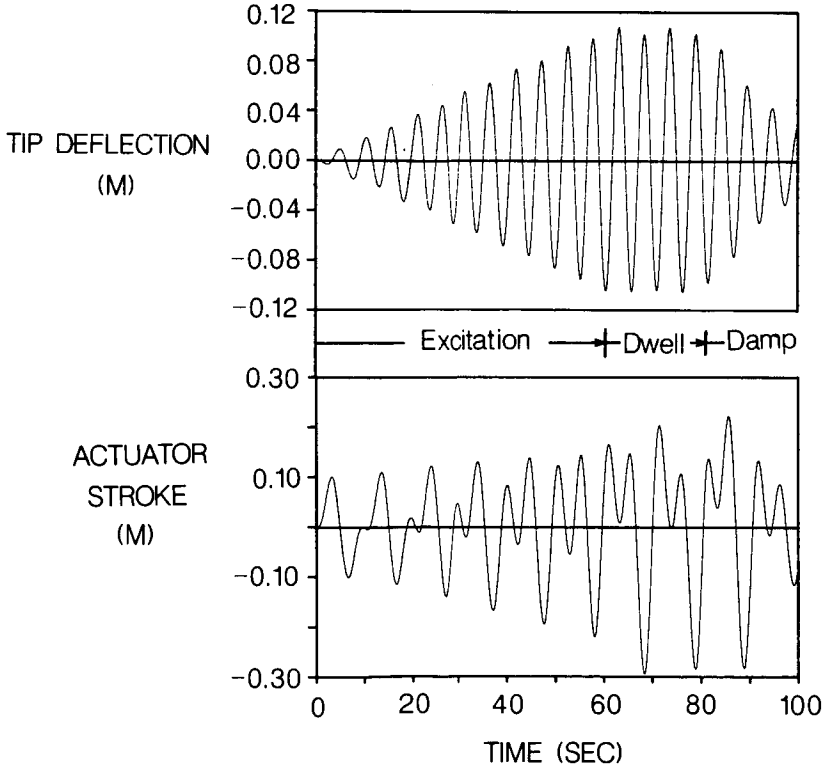

Figure 11

ACTUATOR RESPONSE

The upper plot of figure 12 depicts the force-stroke response corresponding to the excitation of the first bending mode (first 60.4 seconds). The current primary LDCM design provides a maximum force output of 30 N and a maximum stroke of 16 cm (32 cm peak to peak). This simulation shows that for first mode excitation the binding constraint is the maximum stroke. The lower plot shows the actuator force as a function of the beam tip rate during the controlled cycle (last 30 seconds of simulation). In the ideal case this plot is a line with a slope equal to the feedback gain (-6.5 m/s-N). The actuator dynamics causes this distortion.

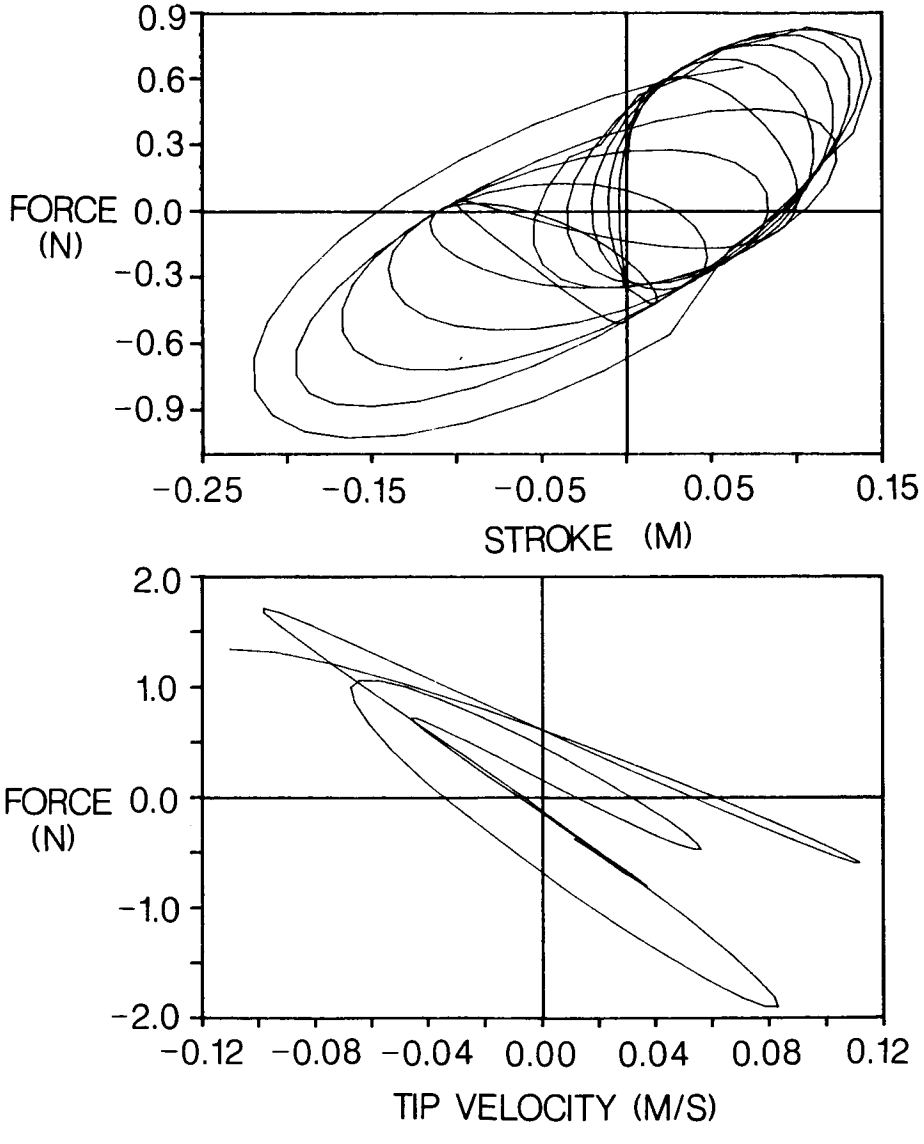

Figure 12

SUMMARY

In-house analysis work in support of the Control of Flexible Structures (COFS) program is being performed at the NASA Langley Research Center. The work involves evaluation of the proposed design configuration, controller design as well as actuator dynamic modeling, and MAST/actuator dynamic simulation for excitation and damping. A complete finite element model of the MAST has been developed. This finite element model has been incorporated into an optimization procedure which minimizes total mass while maintaining modal coupling. Results show an increase in the total mass due to additional constraints (namely, the diagonal frequency constraint) imposed on the baseline design. A valid actuator dynamic model is presented and a complete test sequence of the proposed flight experiment is demonstrated. The actuator dynamic model is successfully used for damping and the stroke limitations for first mode excitation are demonstrated. Plans are to incorporate additional design variables and constraints into the optimization procedure (such as actuator location) and explore alternative formulations of the objective function. A different actuator dynamic model to include hardware limitations will be investigated.

SUMMARY

- MAST FINITE ELEMENT MODEL GENERATED
- OPTIMIZATION PROCEDURE TO INCORPORATE ADDITIONAL DESIGN CONSTRAINTS IS DEMONSTRATED
- ACTUATOR DYNAMIC MODEL SUCCESSFULLY USED FOR EXCITATION AND DAMPING
- COMPLETE TEST SEQUENCE OF THE PROPOSED FLIGHT EXPERIMENT DEMONSTRATED

FUTURE PLANS

- AUGMENT THE OPTIMIZATION PROCEDURE TO INCLUDE PARAMETER MODIFICATION PACKAGE AND ACTUATORS
- INVESTIGATE THE PERFORMANCE OF A DIFFERENT ACTUATOR DYNAMIC MODEL

REFERENCES

1. Hanks, B. R.: "Control of Flexible Structures (COFS) Flight Experiment Background and Description," Large Space Antenna Systems Technology 1984. NASA CP-2368, Part 2, December 1984, pp. 893-902.

2. Horner, G. C.: "COFS-I Program Overview," To be presented at the First NASA/DOD CSI Technology Conference, Norfolk, Virginia, November 18-21, 1986.

3. Whetstone, W. D.: EISI-EAL Engineering Analysis Language Reference Manual - EISI-EAL System Level 2091. Engineering Information Systems, Inc., July 1983.

4. Vanderplaats, Garret N.: CONMIN _ A FORTRAN Program for Constrained Function Minimization - User's Manual. NASA TM X-62282, 1973.

5. Zimmerman, D. C.: "Dynamic Characterization and Microprocessor Control of the NASA/UVA Proof Mass Actuator," M.S. Thesis, University of Buffalo, June 1984.

6. Zimmerman, D. C.; Inman, D.J.; and Horner, G. C.: "Dynamic Characterization and Microprocessor Control of the NASA/UVA/UB Proof Mass Actuator," Proceedings of the 25th AIAA/ASME/ASCE/AHS Structure, Structural Dynamics and Materials Conference. Palm Springs, Ca. May 1984, Paper No. 84-1077.